Hindawi
International Journal of Antennas and Propagation
Volume 2024, Article ID 6410202, 10 pages
https://doi.org/10.1155/2024/6410202

Research Article

Triple-Band MIMO Antenna for 5 G Terminals

Adnane Ghiat,[1] **Abdelwahed Tribak**,[1] **Jaouad Terhzaz**,[2] **Asmae Mimouni**,[3] **and Hanan Akhdar**[3]

[1]*Department of Microwave and Communication Antenna Subsystems, INPT, Rabat, Morocco*
[2]*Department of Physics, CRMEF Casablanca-Settat, Casablanca, Morocco*
[3]*Department of Physics, College of Science, Imam Mohammad Ibn Saud Islamic University (IMSIU), P.O. Box 90950, Riyadh 11623, Saudi Arabia*

Correspondence should be addressed to Adnane Ghiat; adnaneghiat@gmail.com

Received 17 November 2023; Revised 12 February 2024; Accepted 28 February 2024; Published 13 March 2024

Academic Editor: Trushit Upadhyaya

In this work, a triple-band, four-element antenna is designed for fifth-generation (5 G) terminals operating in LTE band 42 (3.4–3.6 GHz), LTE band 43 (3.6–3.8 GHz), and the new 5 G radio band (4.8–5.0 GHz). The proposed antenna array consists of two different types of antenna elements: a T-shaped element, which is connected to the feed line, and a C-shaped element, which is used to divide the bandwidth. The overall size of the proposed antenna element is only 10.5 mm × 5 mm. The multiantenna system has four antennas and is built on a 0.5-mm-thick Rogers 4003C substrate. The results for this antenna show a 10 dB measured bandwidth of 650 MHz at the center frequency of 3.6 GHz and 230 MHz at 4.9 GHz, a gain of more than 4 dBi, an isolation of more than 14 dB, and an overall radiation efficiency of more than 82%.

1. Introduction

Fifth-generation (5 G) mobile communications is the latest wireless technology standard that promises to significantly improve network speed, connectivity, and efficiency over the previous 4 G LTE technology [1, 2]. 5 G technology is expected to enable a wide range of applications, including high-speed Internet access, virtual reality, self-driving cars, and many others classified as Industry 4.0.

Speed is one of the key benefits of 5 G technology. It is designed to deliver data transfer speeds up to 20 times faster than 4 G LTE technology, enabling large file downloads and high-quality video streaming. In addition, 5 G technology offers low latency, which means that data can be transmitted with very little delay, enabling real-time communications and faster response times for applications that require it.

5 G networks use high-frequency radio waves with shorter wavelengths than previous generations of wireless communication technologies to enable high data rates and minimal latency. To enable the use of these high-frequency radio waves, 5 G antennas must be designed to operate at these frequencies and handle the high data rates expected from 5 G technology. They also need to be tiny and compact to easily fit into the design of 5 G terminals such as smartphones, tablets, and other mobile devices.

5 G antennas will increase signal strength and overall network performance by using advanced technologies such as beamforming [3] and multiple-input, multiple-output (MIMO). Beamforming allows the antenna to focus the signal in a specific direction, improving signal power and quality, while MIMO allows the use of four or more antenna systems instead of a single antenna for signal transmission and reception, further improving signal quality and overall network performance. However, the compactness of the mobile terminal presents some challenges, such as antenna miniaturization, improved antenna isolation, and lower envelope correlation coefficient (ECC).

In an attempt to minimize the dimensions of the antenna, Liu et al. [4, 5] have chosen to extend the current path of the resonator by slitting, while Sun et al. [6, 7] have chosen to bend the current path. Unfortunately, this approach leads to current cancellation and a consequent reduction in gain. Liu et al.

propose an alternative method, advocating the incorporation of energy storage components such as inductors [8] and capacitors [9]. This not only helps minimize the size of the antenna but also allows for easy tuning of the resonant frequency. Another approach, described in references [10, 11], involves Xing et al. using a different substrate material (ceramic) with a higher dielectric constant. It is worth noting, however, that this choice is made at the expense of the antenna's bandwidth.

In an effort to improve antenna isolation, Ren and Zhao in [12] adopt a self-decoupled structure, while Guo et al. in [13] use a neutralization line, and Chang et al. in [14] pursue orthogonal polarization to reduce coupling between adjacent antenna elements and achieve improved antenna isolation. In addition, high-impedance surfaces (HIS) in [15] and metamaterial structures in [16] are used to attenuate surface waves and decouple antenna elements. Despite the effectiveness of these decoupling techniques, the transition from a basic MIMO system to a massive MIMO system requires additional measures.

In this research, we introduce a new triple-band sub-6 GHz 5 G four-element MIMO antenna system for mobile terminals with a specific frequency range. The four-antenna array consists of two dual-antenna arrays printed perpendicularly on both side frames of the main substrate, where the feed line and ground plane are printed. The proposed MIMO antenna system can cover the entire trio of bands: 3.5 GHz (3.4–3.6 GHz), 3.7 GHz (3.6–3.8 GHz), and 4.9 GHz (4.8–5.0 GHz), which are licensed by the U.S., Japan, and China, respectively, for 5 G applications [17, 18].

2. Proposed Antenna Array

2.1. Antenna Design. Figure 1 and Table 1 depict the geometry of the proposed 4-antenna MIMO system for use in a mobile terminal. The dimensions of the system substrate are 150 mm × 74 mm × 0.5 mm (the size of a typical smartphone), and the ground plane has the same dimensions with a G clearance along the two side edges of the system substrate. Two tiny antenna pairs are individually mounted on two antenna frames on the left and right sides of the phone (similar to the antenna configurations proposed in [13, 19]). The 150 mm × 5 mm × 0.5 mm antenna frames are perpendicularly attached to the system substrate at a height of $N = 1$ mm. The system substrate and antenna frames are made of Rogers 4003C with a relative permittivity of 3.55 and a dissipation factor of 0.0021. Each antenna element is located 58 mm from the center of the antenna frame. A single antenna element occupies a total area of 10.5 mm × 5 mm, and each array element consists of a T-shaped radiating branch connected to a 50 Ω feed strip, a C-shaped structure on the front of the frame acting as a frequency divider, and all antennas are fed by 50 Ω SMA connectors through a hole on the back of the system substrate. The exact dimensions of the antenna are shown as follows.

Initially, the feed branch, which is connected to an SMA connector, has LF = 10 mm and WF = 0.8 mm, indicating its length and width; the end of the feed branch is directly connected to a T-shaped radiating branch printed on the back of the frame; a C-shaped element is printed on the opposite side of the frame; and it has no connection to any other part of the antenna.

2.2. Antenna Analysis

2.2.1. Evolution Process. The design evolution and parameter analysis of the antenna element have all been investigated to better comprehend the mechanism of the proposed MIMO antenna system.

In Case 1 of Figures 2 and 3, a simple inner-branch monopole is connected to the feed line. In Case 2, a horizontal inner strip is added to the top of the monopole to form a T-shaped strip. The antenna in Case 2, which only consists of a T-shaped radiation pattern, has the characteristics of a wide single band (with more than 1.1 GHz bandwidth) with 4 GHz as the center frequency. The construction of the antenna in Case 3 involves adding a C-shaped structure on the outside of the frame to the components of the antenna in Case 2. Now, because of the added structure, the antenna has two different frequency resonances at 3.6 and 4.6 GHz, but that is not what we are looking for; the antenna requires a slight adjustment in parameters to achieve the desired bands. By adjusting the size of its lower leg, the second resonance point changes. The proposed antenna, capable of providing full coverage of the 3.4 to 3.8 GHz and 4.8 to 5 GHz frequency bands, is the result of reducing the length of the lower leg.

2.2.2. The Impact of the Novel Split Bandwidth. The introduction of a C-shaped structure, which is independent of both the feed line and the radiating element (as opposed to the concept in [20, 21], which uses a via connection between different layers), reveals a remarkable split-bandwidth capability. This innovative design represents a significant leap forward in antenna technology. With this unique configuration, antennas can operate at multiple frequencies simultaneously, greatly enhancing their adaptability and performance. This breakthrough has far-reaching implications, especially for industries that rely on wireless communications. It promises higher data rates, reduced interference, and improved network reliability. The C-shaped independent structure is a testament to the progress being made in advancing antenna technology and heralds a future of even more efficient and reliable wireless connectivity. Figure 4 illustrates how adjusting the new parameters affects the antenna design.

The antenna current distributions and radiation patterns can be used to better understand the behavior of the proposed antenna element as illustrated in Figures 5 and 6. When the proposed antenna is activated, the two low-band current distributions (3.5 GHz and 3.7 GHz) are concentrated on one side of the T-shaped branch of the antenna, while the high-band current distribution (4.9 GHz) is mostly concentrated on the C-shaped branch of the antenna. This shows that in the low bands (3.5 GHz and 3.7 GHz), the currents remain on the branch connected to the feed line, but in the high bands (4.9 GHz), the currents practically penetrate the frame and move from the T-shaped branch to the C-shaped branch. This feature ensures the multiband function of the antenna and the importance of the C-shaped structure.

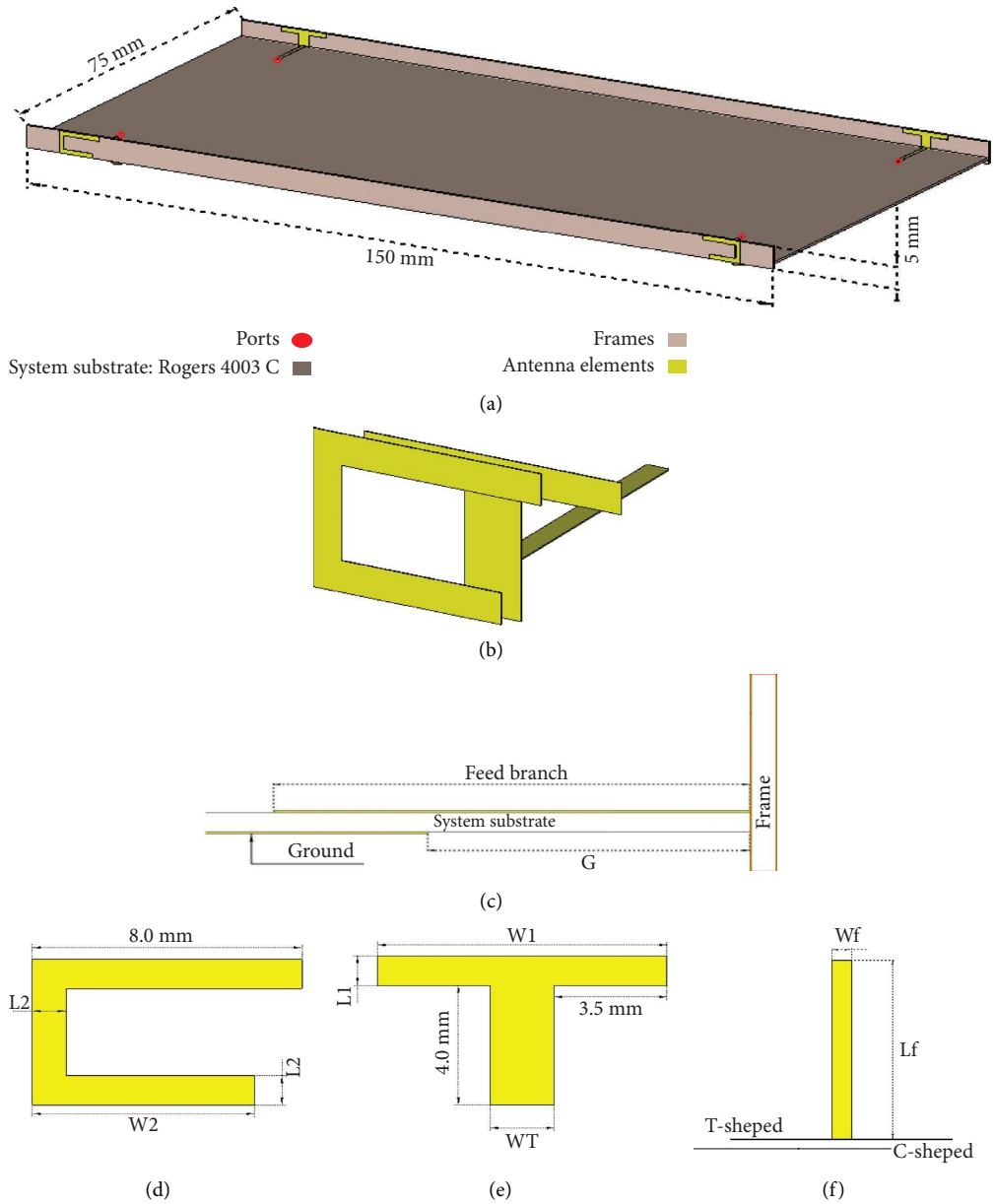

Figure 1: Geometry of the triple-band 4-antenna MIMO system. (a) Global structure. (b) One element. (c) Left view. (d) Front view. (e) Back view. (f) Top view.

Table 1: Antenna dimension.

Parameter	Value (mm)
L1	1
W1	9
L2	1
W2	6.6
Lf	10
Wf	0.8
WT	2
G	7

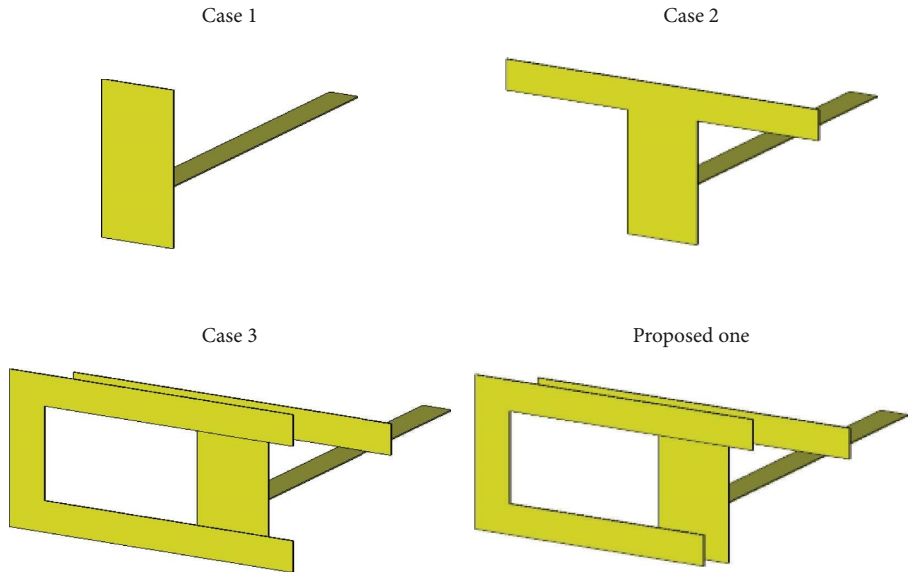

Figure 2: Design evolution of a single antenna.

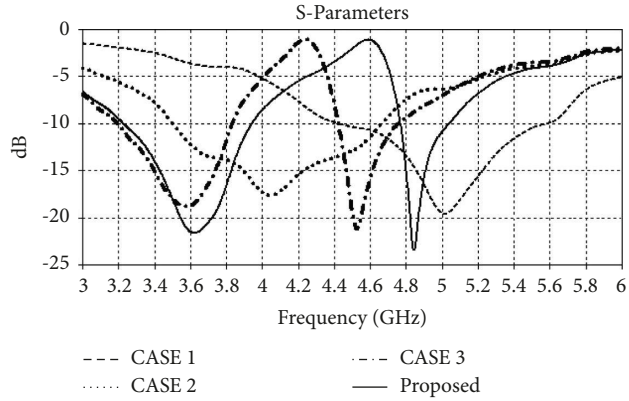

Figure 3: The reflection coefficient for each case.

3. Four Element (MIMO) Antenna Design and Results

The proposed antenna is used to construct a MIMO antenna array to achieve the performance and data throughput requirements of fifth-generation technology. Four antennas are positioned along two side frames to represent the 4-element antenna array, as shown in Figure 7. Antennas on the same side are spaced 116 mm apart, leaving enough space for additional designs. To reduce mutual interference between antennas on different sides, two 50×0.4 mm gaps are made in the ground plan to isolate the coupling current from one antenna to the other.

In order to smoothly integrate the proposed MIMO structure into mobile phones, a parametric study of its overall dimensions is crucial. The primary goal is to downsize the structure while maintaining or improving its performance metrics. This downsizing initiative is aimed at optimizing the compatibility of the MIMO structure with the compact form factor of handheld devices. Figure 8 illustrates the comparison of systematically adjusting various parameters such as element spacing, ground plan dimensions, and overall antenna array dimensions by −4% and −8%. By carefully analyzing the effects of these parameter variations through simulation, we can ensure that the downsized MIMO structure meets the stringent size constraints of handheld phones while providing reliable and efficient wireless communication capabilities.

3.1. Performance of the MIMO Antenna System. In Figure 9, we built a prototype of the proposed 4-antenna MIMO system. We performed S11 measurements using the Agilent N3383A vector network analyzer (VNA), which was calibrated in the frequency range of 300 kHz to 9 GHz using the Agilent 85033E 3.5 mm calibration kit. Then, we evaluated its performance by comparing the experimental results with simulations obtained from two different programs: CST and Ansys HFSS. Remarkably, the comparison yielded almost identical results.

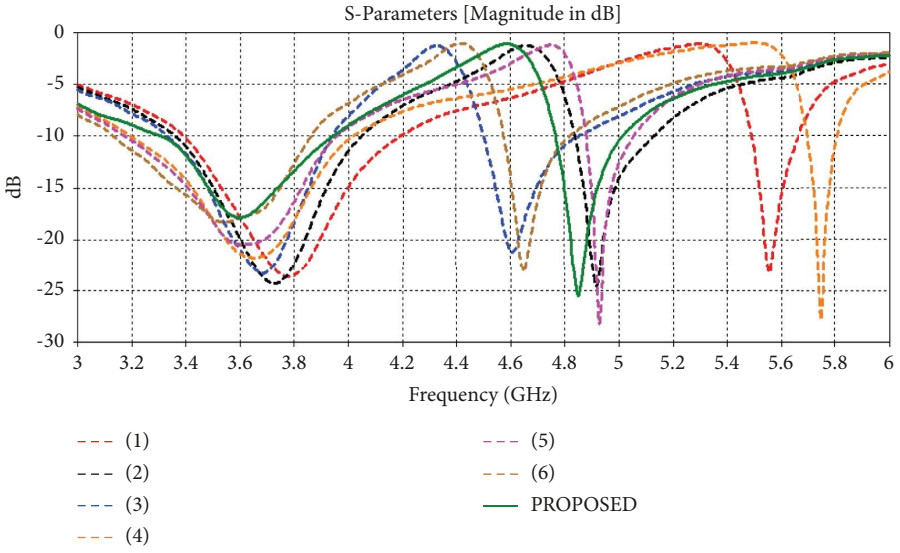

S1,1	L2 (mm)	W3 (mm)	W2 (mm)
1	0.5	6	6
2	0.5	7	7
3	0.5	8	8
4	1.5	6	6
5	1.5	7	7
6	1.5	8	8
Proposed	1	8	6.6

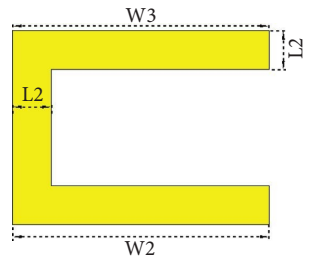

Figure 4: Analyzing the parameters of the innovative split bandwidth structure.

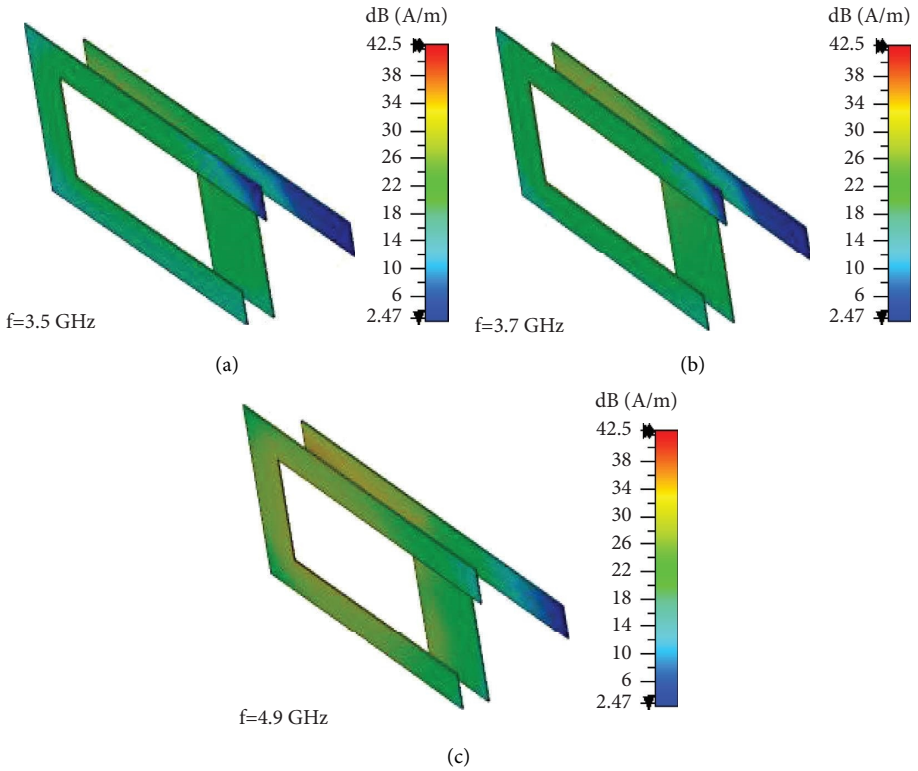

Figure 5: Simulated current distributions at (a) 3.5 GHz. (b) 3.7 GHz. (c) 4.9 GHz.

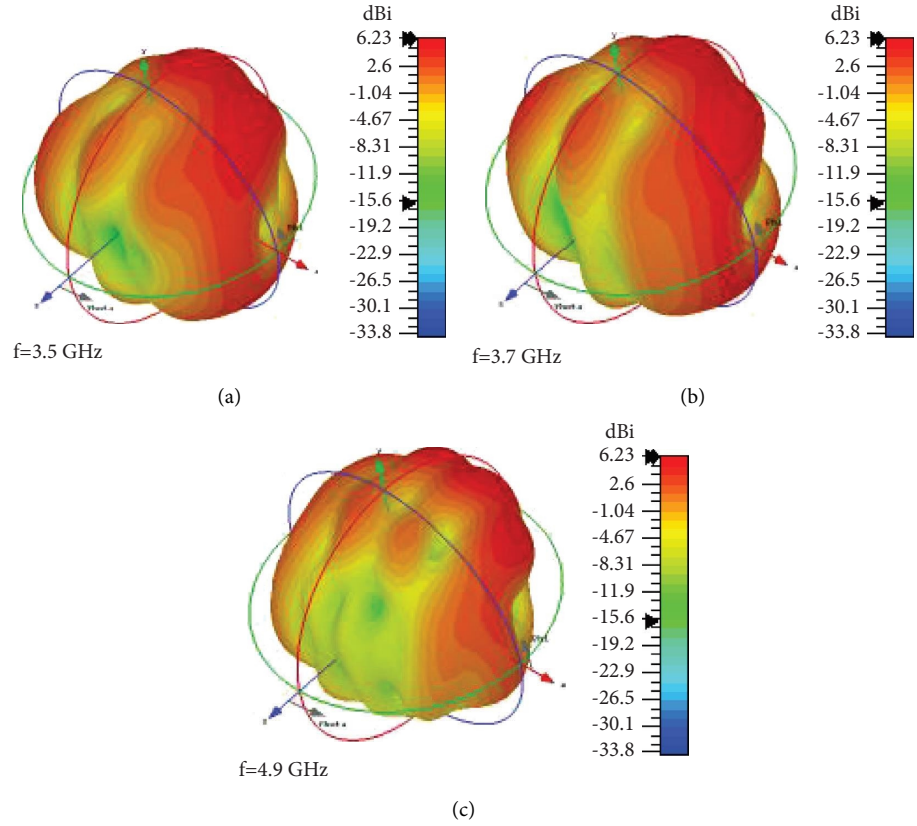

Figure 6: 3D radiation patterns of the proposed antenna element at (a) 3.5 GHz. (b) 3.7 GHz. (c) 4.9 GHz.

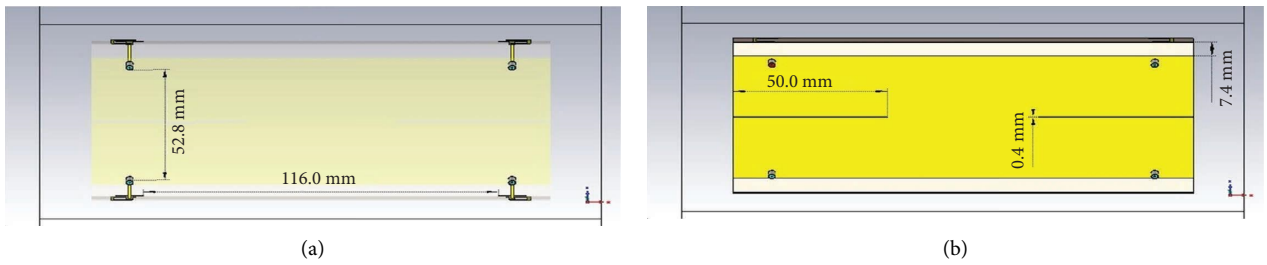

Figure 7: (a) The exact location of the four antennas. (b) Size of the two slots in the ground plan.

The impedance bandwidth represented by S11 in Figure 10 shows that the proposed MIMO antenna system can fully cover LTE bands 42 (3.4–3.6 GHz) and 43 (3.6–3.8 GHz), in addition to the 5 G New Radio band of 4.8–5.0 GHz. One of the key issues that can significantly affect the performance of MIMO wireless systems is the mutual coupling between MIMO antenna elements. Therefore, it is usually necessary to use an efficient decoupling technique for the closely spaced MIMO antennas. The effect of coupling on the proposed triple-band MIMO antenna has been investigated in Figures 11 and 12. There is no problem with the isolation between ports 1, 2, and 4, represented by S1, 2 and S1, 4, respectively. However, due to their close proximity, which is exactly 52.8 mm, and the sheared ground plan, ports 1 and 3 have a mutual coupling of about 10 dB. This is where the two slots in the ground plane come into play, as shown in Figure 7. The mutual coupling improved with these slots, especially in the mid-band (3.6–3.8 GHz), where it went from 10 dB to 14 dB, which is a big improvement.

Furthermore, in Figures 13 and 14, the antenna realized gains are 4.9 dBi at 3.5 GHz, 4.8 dBi at 3.7 GHz, and 5.8 dBi at 4.9 GHz, with the total efficiency ranging from 82% to 89% in all bands. The gain and efficiency of the antenna system show its strength.

Figure 15 displays the Envelope Correlation Coefficients (ECC) of the proposed MIMO antenna system. The ECC values are estimated based on the complex radiation farfields for each pair of antennas (i) and (j) using the following equation [20]:

Structure	*W*	*L*	*Curve*
Proposed	*150*	*75*	*(1)*
Downsize (4%)	*144*	*72*	*(2)*
Downsize (8%)	*138*	*69*	*(3)*

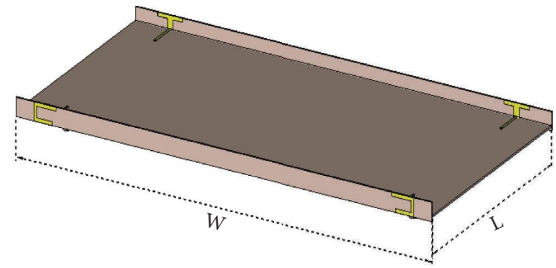

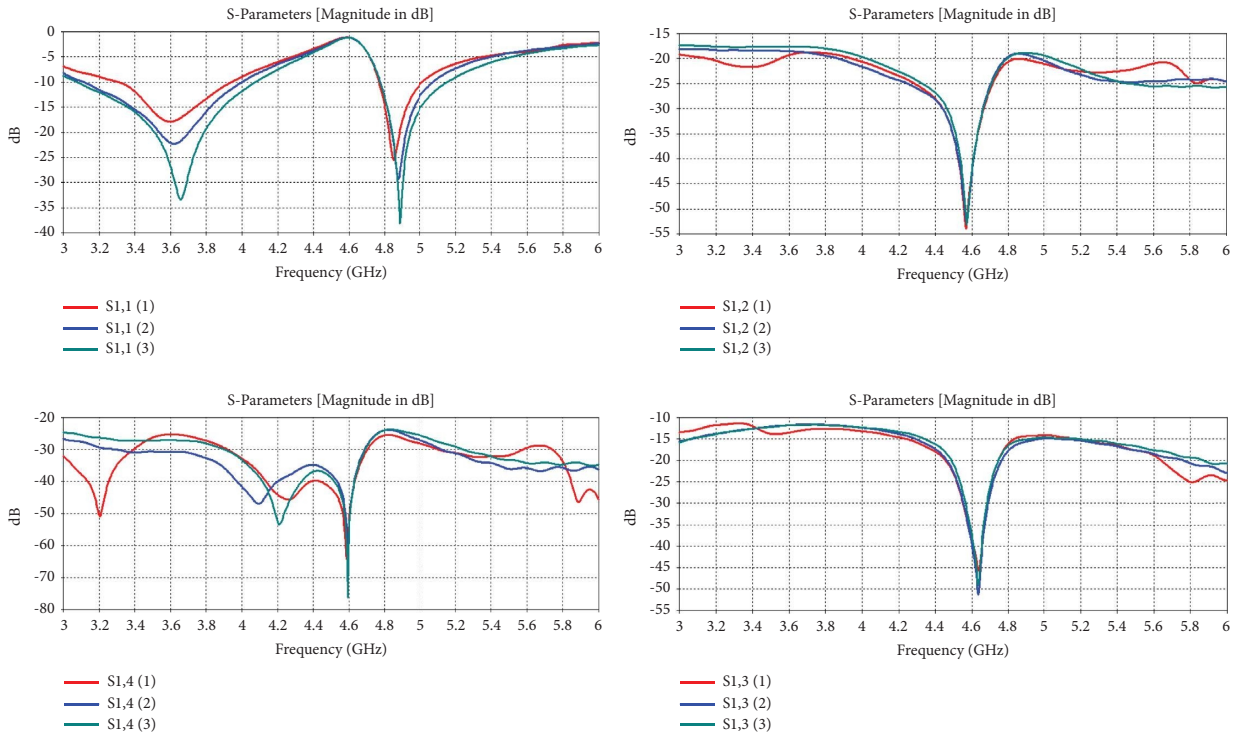

Figure 8: Analyzing the *S*-parameters of downsized MIMO structure.

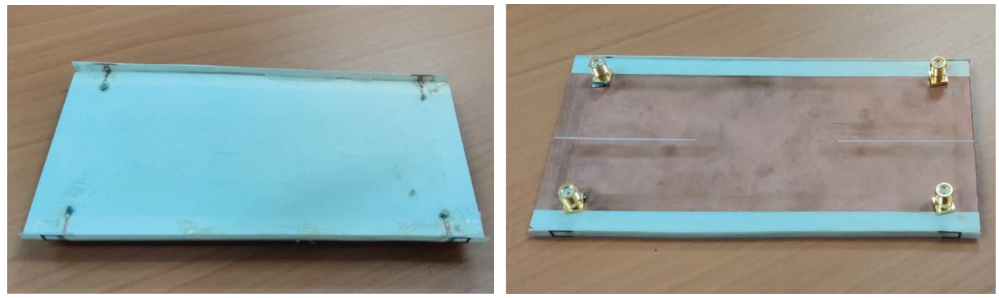

Figure 9: Prototype of the proposed 4-antenna MIMO system.

$$\mathrm{ECC}(i,j) = \frac{\left|\oiint A_{ij}(\theta,\phi)\sin\theta d\theta\, \mathrm{d}\phi\right|^2}{\oiint A_{ii}(\theta,\phi)\sin\theta d\theta\, \mathrm{d}\phi . \oiint A_{jj}(\theta,\phi)\sin\theta d\theta\, \mathrm{d}\phi}, \quad (1)$$

where

$$A_{ij}(\theta,\phi) = E_{\theta,i}(\theta,\phi).E^*_{\theta,j}(\theta,\phi) + E_{\phi,i}(\theta,\phi).E^*_{\phi,j}(\theta,\phi). \quad (2)$$

(i) $A_{ij}(\theta,\phi)$ is the antenna pattern between antennas i and j. (ii) $A_{ii}(\theta,\phi)$ is the antenna pattern of antenna i. (iii) $A_{jj}(\theta,\phi)$ is the antenna pattern of antenna j. (iv) The integrals are over the solid angle, with θ representing the elevation angle and ϕ representing the azimuth angle.

These values reflect the degree of isolation between the antennas. The ECC values in band 42 and the high band are less than 0.02 and ECC (1, 4) is the higher one, while in the

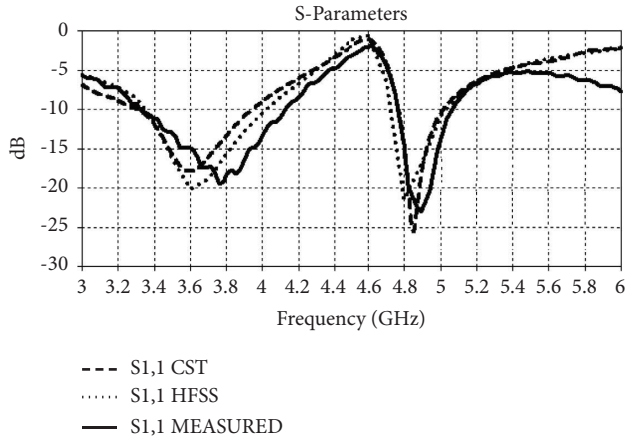

Figure 10: Simulated and measured reflection coefficients for the proposed 4 antenna MIMO system.

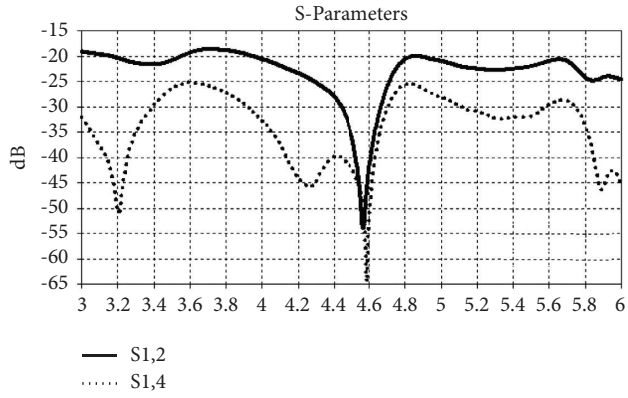

Figure 11: The mutual coupling between ports 1, 2, and 4.

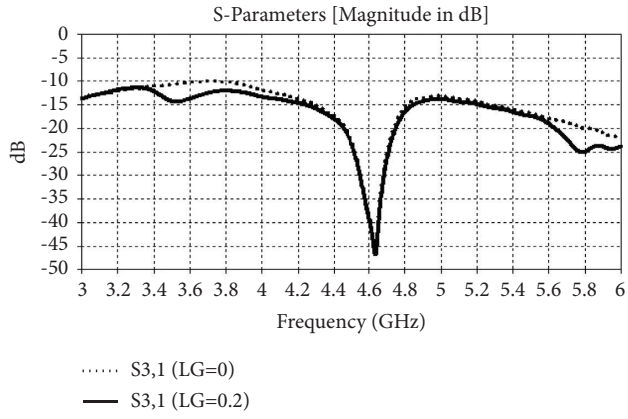

Figure 12: The mutual coupling between ports 1 and 3 (with/without) ground gaps.

middle band, they are less than 0.01 and ECC (1, 2) is the higher one; these results indicate better spatial separation between the antennas, allowing them to capture more independent information from the environment. This spatial

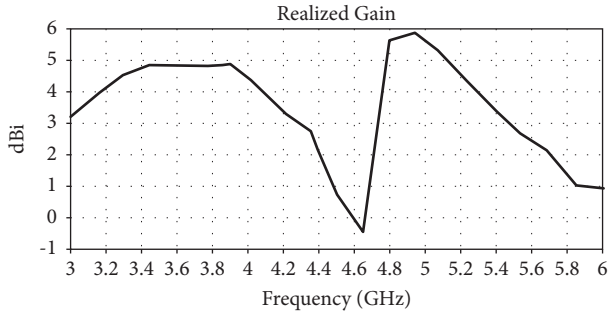

Figure 13: Antenna realized gain.

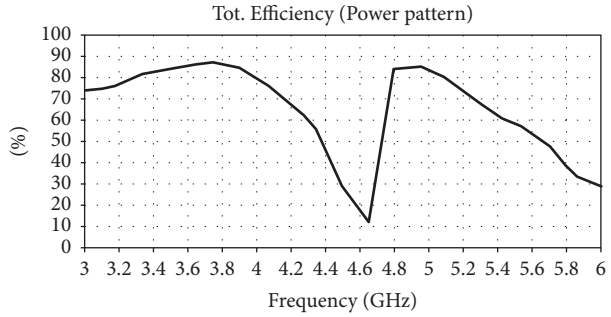

Figure 14: Total efficiency of the antenna system.

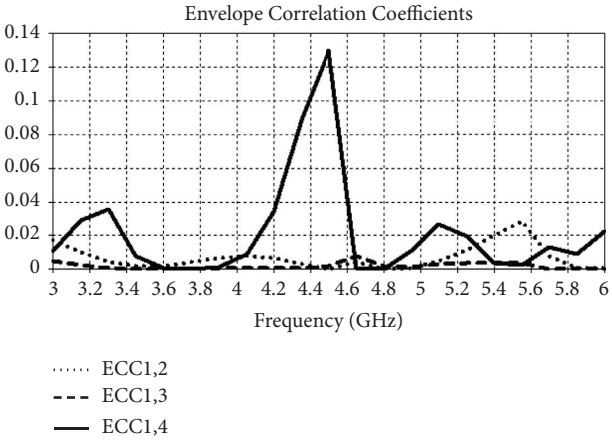

Figure 15: ECCs for the proposed MIMO antenna system.

separation is crucial for achieving spatial multiplexing gains in MIMO systems, where multiple data streams are transmitted simultaneously on different antennas.

Table 2 highlights and compares the performance of the proposed design with the results of various existing designs. The proposed design clearly outperforms in terms of both efficiency and envelope correlation coefficient (ECC), thanks to the optimization of the shape, size, and configuration of the radiating element, along with higher-than-average isolation. In addition, the proposed design deviates from conventional approaches by covering three bands.

Table 2: Performance comparison of antennas for 5 G applications.

Reference	Operating band (GHz)	Isolation (dB)	ECC	Efficiency (%)	Element size (mm^2)
[22]	[3.3–4.2][4.8–5]	>10	<0.1	53.8–79.1	18.6 × 7
[23]	[3.3–6]	>12.8	<0.06	>50	11.4 × 8.4
[24]	[3.3–3.6][4.8–5]	>12	<0.15	>45	10.6 × 5.3
[25]	[3.3–6]	>11.4	<0.26	>46	14.5 × 1.5
[26]	[3.4–3.8]	>14.8	<0.05	>74	18.2 × 7.5
[27]	[3.3–3.6][5.1–5.9]	>11.2	<0.08	51–59	10 × 10
[28]	[3.3–3.8]	>10	<0.2	>58	14.5 × 1.5
[29]	[3.4–3.6]	>10	<0.3	45–60	14 × 8
[30]	[4.5–5]	>15	<0.02	N/A	6 × 12
[31]	[3.3–6]	>10	<0.1	40–70	13.9 × 7
[32]	[3.4–3.6]	>12	<0.2	42–65	12.5 × 18.5
[33]	[3.3–3.6] [4.8–5]	>10	<0.38	>36	15 × 3
Proposed one	[3.4–3.6][3.6–3.8][4.8–5]	>14	<0.02	82–89	10.5 × 5

4. Conclusion

In this article, a 4-element (MIMO) antenna array is designed specifically for 5 G terminals. The proposed antenna can fully cover all three different 5 G frequency bands: [3.4 GHz–3.6 GHz], [3.6 GHz–3.8 GHz], and [4.8 GHz–5 GHz]. The antenna array is designed to provide several desirable features, including high gain over 4 dBi, which allows the signal to be transmitted over long distances with little loss of signal strength. In addition, it offers high isolation above 14 dB, meaning that the signals sent by one antenna element will not interfere with those sent by other components in the array. This feature is particularly important for 5 G systems, where multiple antennas will be used simultaneously. The proposed antenna array also exhibits high efficiency, exceeding 82%. Finally, the ECC is less than 0.02.

Due to its robust MIMO performance, the proposed antenna is expected to be used in various 5 G mobile communication applications, especially those that require high-speed data transfer, low latency, and reliable transmission.

Data Availability

The PROJECT1.RAR data used to support the findings of this study have been attached with the article.

Conflicts of Interest

The authors declare that there are no conflicts of interest regarding the publication of this paper.

Authors' Contributions

Conceptualization, investigation, and writing original draft preparation were conducted by A. Ghiat; methodology and validation were performed by A. Ghiat and J. Terhzaz; resources were collected by A. Mimouni and H. Akhdar; writing, review, and editing were carried out by A. Tribak and J. Terhzaz; visualization was performed by A. Ghiat, A. Tribak, and J. Terhzaz.; supervision and project administration were conducted by A. Tribak. All authors have read and agreed to the published version of the manuscript.

Acknowledgments

The authors would like to thank the Deanship of Science Research at Imam Mohammad Ibn Saud Islamic University for their funding under Research Group no. RG-21-09-47 and Mr. Tomás Fernández from the Department of Communications Engineering of the University of Cantabria for his software support.

References

[1] L. B. Le, V. Lau, E. Jorswieck et al., *Enabling 5G mobile Wireless Technologies*, SpringerOpen, Berlin, Germany, 2015.

[2] J. G. Andrews, S. Buzzi, W. Choi et al., "What will 5G be?" *IEEE Journal on Selected Areas in Communications*, vol. 32, no. 6, pp. 1065–1082, 2014.

[3] W. Hong, Z. H. Jiang, C. Yu et al., "The role of millimeter-wave technologies in 5G/6G wireless communications," *IEEE Journal of Microwaves*, vol. 1, no. 1, pp. 101–122, 2021.

[4] Y. Liu, A. D. Ren, H. Liu, H. Y. Wang, and C. Y. D. Sim, "Eight-Port MIMO array using characteristic mode theory for 5G smartphone applications," *IEEE Access*, vol. 7, pp. 45679–45692, 2019.

[5] Y. X. Li, C. Y. D. Sim, Y. Luo, and G. L. Yang, "High-isolation 3.5 GHz eight-antenna MIMO array using balanced open-slot antenna element for 5G smartphones," *IEEE Transactions on Antennas and Propagation*, vol. 67, no. 6, pp. 3820–3830, 2019.

[6] L. Sun, Y. Li, Z. Zhang, and Z. Feng, "Wideband 5G MIMO antenna with integrated orthogonal-mode dual-antenna pairs for metal-rimmed smartphones," *IEEE Transactions on Antennas and Propagation*, vol. 68, no. 4, pp. 2494–2503, 2020.

[7] W. Hu, L. Qian, S. Gao et al., "Dual-band eight-element MIMO array using multi-slot decoupling technique for 5G terminals," *IEEE Access*, vol. 7, pp. 153910–153920, 2019.

[8] Y. Liu, W. Cui, Y. T. Jia, and A. D. Ren, "Hepta-band metal-frame antenna for LTE/WWAN full-screen smartphone," *IEEE Antennas and Wireless Propagation Letters*, vol. 19, no. 7, pp. 1241–1245, 2020.

[9] Z.-Q. Xu, Q.-Q. Zhou, Y.-L. Ban, and S. S. Ang, "Hepta-band coupled-fed loop antenna for LTE/WWAN unbroken metal-rimmed smartphone applications," *IEEE Antennas and Wireless Propagation Letters*, vol. 17, no. 2, pp. 311–314, 2018.

[10] L. Xing, Y. Huang, Q. Xu, S. Alja'afreh, and T. Liu, "A broadband hybrid water antenna for hand-portable applications," *IEEE Antennas and Wireless Propagation Letters*, vol. 15, pp. 174–177, 2016.

[11] L. Xing, Y. Huang, Q. Xu, and S. Alja'afreh, "A transparent dielectric-loaded reconfigurable antenna with a wide tuning range," *IEEE Antennas and Wireless Propagation Letters*, vol. 15, pp. 1630–1633, 2016.

[12] Z. Y. Ren and A. P. Zhao, "Dual-band MIMO antenna with compact self-decoupled antenna pairs for 5G mobile applications," *IEEE Access*, vol. 7, pp. 82288–82296, 2019.

[13] J. L. Guo, L. Cui, C. Li, and B. H. Sun, "Side-edge frame printed eight-port dual-band antenna array for 5G smartphone applications," *IEEE Transactions on Antennas and Propagation*, vol. 66, no. 12, pp. 7412–7417, 2018.

[14] L. Chang, Y. F. Yu, K. P. Wei, and H. Y. Wang, "Orthogonally polarized dual antenna pair with high isolation and balanced high performance for 5G MIMO smartphone," *IEEE Transactions on Antennas and Propagation*, vol. 68, no. 5, pp. 3487–3495, 2020.

[15] X. Jiang, H. Wang, and T. Jiang, "A low mutual coupling MIMO antenna using EBG structures," in *Proceedings of the 2017 Progress In Electromagnetics Research Symposium-Spring (PIERS)*, IEEE, St. Petersburg, Russia, May 2017.

[16] S. R. Thummaluru and R. K. Chaudhary, "Mu-negative metamaterial filter-based isolation technique for MIMO antennas," *Electronics Letters*, vol. 53, no. 10, pp. 644–646, 2017.

[17] Qualcomm, "5G NR (new radio)," 2023, https://www.qualcomm.com/research/5g/5g-nr.

[18] Asia Times, "China reserves spectrum for 5G services," 2023, https://asiatimes.com/2017/11/china-reserves-spectrum-5gservices/.

[19] R. Li, Z. Mo, H. Sun, X. Sun, and G. Du, "A low-profile and high-isolated MIMO antenna for 5G mobile terminal," *Micromachines*, vol. 11, no. 4, pp. 360–2020, 2020.

[20] Z. Y. Ren, A. P. Zhao, and S. J. Wu, "MIMO antenna with compact decoupled antenna pairs for 5G mobile terminals," *IEEE Antennas and Wireless Propagation Letters*, vol. 18, no. 7, pp. 1367–1371, 2019.

[21] Y. J. Zhang, Y. Li, M. Z. Hu, P. F. Wu, and H. Y. Wang, "Dual-band circular-polarized microstrip antenna for ultra-wideband positioning in smartphones with flexible liquid crystal polymer process," *IEEE Transactions on Antennas and Propagation*, vol. 71, no. 4, pp. 3155–3163, 2023.

[22] L. Cui, J. L. Guo, Y. Liu, and C. Y. D. Sim, "An 8-element dual-band MIMO antenna with decoupling stub for 5G smartphone applications," *IEEE Antennas and Wireless Propagation Letters*, vol. 18, no. 10, pp. 2095–2099, 2019.

[23] M. M. Fakharian, "A low-profile compact UWB antenna array for sub-6 GHz MIMO applications in 5G metal-frame smartphones," *International Journal of RF and Microwave Computer-Aided Engineering*, vol. 32, no. 10, Article ID e23320, 2022.

[24] J. Huang, G. Dong, Q. Cai, Z. Chen, L. Li, and G. Liu, "Dual-band MIMO antenna for 5G/WLAN mobile terminals," *Micromachines*, vol. 12, no. 5, pp. 489–2021, 2021.

[25] Z. Liu, H. Liu, D. W. Huang, and Z. W. Du, "Wideband antenna pair and its applications for 5G metal frame mobile phones," *Journal of Electromagnetic Waves and Applications*, vol. 35, no. 13, pp. 1742–1753, 2021.

[26] V. Thakur, N. Jaglan, and S. D. Gupta, "Design of a dual-band 12-element MIMO antenna array for 5G mobile applications," *Progress in Electromagnetics Research Letters*, vol. 95, pp. 73–81, 2021.

[27] J. X. Li, X. K. Zhang, Z. Wang et al., "Dual-band eight-antenna array design for MIMO applications in 5G mobile terminals," *IEEE Access*, vol. 7, pp. 71636–71644, 2019.

[28] C. Huang and J. Sui, "High-Isolated multi-element MIMO antennas for mobile terminals," in *Proceedings of the 2022 IEEE Conference on Antenna Measurements and Applications (CAMA)*, IEEE, Guangzhou, China, December 2022.

[29] S. H. Kiani, A. Altaf, M. Abdullah et al., "Eight element side edged framed MIMO antenna array for future 5G smart phones," *Micromachines*, vol. 11, no. 11, pp. 956–2020, 2020.

[30] R. K. Jaiswal, K. Kumari, A. K. Ojha, and K. V. Srivastava, "Five-port MIMO antenna for n79-5G band with improved isolation by diversity and decoupling techniques," *Journal of Electromagnetic Waves and Applications*, vol. 36, no. 4, pp. 542–556, 2022.

[31] H.-Y. Liu and C.-J. Huang, "Wideband MIMO antenna array design for future mobile devices operating in the 5G NR frequency bands n77/n78/n79 and LTE band 46," *IEEE Antennas and Wireless Propagation Letters*, vol. 19, no. 1, pp. 74–78, 2019.

[32] S. H. Kiani, A. Altaf, M. R. Anjum et al., "MIMO antenna system for modern 5G handheld devices with healthcare and high rate delivery," *Sensors*, vol. 21, no. 21, pp. 7415–2021, 2021.

[33] C. C. Lin, S. H. Cheng, S. C. Chen, and C. S. Wei, "Compact sub 6 GHz dual band twelve-element MIMO antenna for 5G metal-rimmed smartphone applications," *Micromachines*, vol. 14, no. 7, pp. 1399–2023, 2023.